5.4

CALIBRATION AND USE OF SITE-SPECIFIC URBAN WEATHER OBSERVATIONS DATA USING MICROSCALE MODELING

William J. Coirier *, Sura Kim, Shawn C. Ericson, Saikrishna Marella
CFD Research Corporation, Alabama

1. INTRODUCTION

As noted in [Oke], meteorological weather stations located in urban areas often yield unusable and unreliable data due to their proximity to buildings and other obstructions. Direct import of this data into Numerical Weather Prediction (NWP) and Atmospheric Transport and Dispersion (ATD) as well as Urban Area Transport and Dispersion (UATD) models is problematic since the individual site readings represent highly localized behavior, and often do not characterize the neighborhood and grid scale meteorological conditions needed by the models. Due to the localized flow and turbulence characteristics caused by the unique obstructions near each intra-urban site location, established siting procedures [WMO, 1983.a,b] cannot be followed [Oke]. These issues have not stopped the propagation of many intra-urban sited weather stations, as evidenced by DCNet [http://dcnet.atdd.noaa.gov/] and even WeatherBug [http://www.WeatherBug.com/].

Recent field tests, such as the Urban 2000 [Allwine, et al., 2002], Joint Urban 2003 [Allwine et al., 2004] and the Department of Homeland Security, Urban Dispersion Program (DHS UDP) sponsored tests in New York City (MSG05 and MID05) [UDP, Hanna et al., 2006], have taken considerable data deep in the urban street canyons. A common premise behind these tests is to take meteorological data readings deep within urban cityscapes that may be used to help improve the accuracy of urban area transport and dispersion models. The use of this data as input into transport and dispersion models is problematical, which is a deficiency we are addressing with this work. As noted in [Coirier, et al., 2006.a], meteorological data taken in urban areas and elsewhere often does not provide sufficient information to be used as input to transport and dispersion models, especially those based upon diagnostic and CFD models.

corresponding author address:
CFD Research Corporation,
215 Wynn Dr., 5th Floor, Huntsville, AL 35805
e-mail: wjc@cfdrc.com.

In this paper we explore and demonstrate a technique based upon using high-resolution Computational Fluid Dynamics (CFD) model output to provide a means to calibrate, correlate and potentially optimize intra-urban weather station sites so that their readings may more appropriately represent the prevailing climatological conditions. We base our study upon the meteorological data taken during the Joint Urban 2003 (JU2003) Field Test in Oklahoma City [Allwine et al., 2004], where a number of wind sensors were located deep in the Central Business District area. We show that by using the approaches presented here, we are able to use the meteorological station data to provide improved boundary condition data to CFD and other models.

The approach investigated here constructs "best fit wind fields" by minimizing a functional that relates the difference between measured (meteorological station) and computed (CFD) data. The CFD data is pre-computed for a range of prevailing conditions, and stored in a database, or "wind library". The use of wind field libraries is gaining popularity and attention, as it provides a means of providing the accuracy and high-fidelity of Computational Fluid Dynamics modeling at extremely low latency [Boris, 2004, Smith, et al., 2002].Once the best fit wind fields are found by performing the minimization approach, correlations between data taken at given meteorological station sites and other locations in the city are readily constructed. These correlations may be used to relate street level winds to rooftop level readings, as well as correlating the station readings with the prevailing conditions. During the construction of the best fit wind fields by the functional minimization, response surfaces are generated which relate the local meteorological stations response to changes in the prevailing conditions by using the high-resolution CFD data stored in the wind library database.

In the following sections we summarize recent progress on how to construct the best fit wind fields using the response surface approach, and demonstrate the overall concept by using data taken during the Joint Urban 2003 (JU2003) field test. First we describe the CFD model used to generate the wind libraries, how we construct the response surfaces and how we use the response surfaces to construct the best fit wind fields. Next, we demonstrate the approach for three Intensive Operating Periods (IOPs) during the Joint Urban 2003 test, followed by demonstrations of how one may use the best fit and response surface data to correlate and characterize sensor response in the urban area.

2. CONSTRUCTION OF THE BEST FIT WINDFIELDS

Our approach uses libraries of high-resolution wind and turbulence fields produced using Computational Fluid Dynamics (CFD) along with intra-urban sited meteorological stations data in order to construct corresponding wind fields that minimize the difference between the measured (meteorological station) and constructed ("best fit") fields. To demonstrate this approach we use the steady-state Reynolds-Averaged Navier-Stokes solutions produced using the CFD-Urban model [Coirier, et al., 2006.b], although the approach may be readily extended to other models including unsteady RANS, LES and even diagnostic models. Given the time-varying meteorological stations readings, the best fit approach produces a representative wind field at each of the sample times, resulting in a pseudo-unsteady wind library that may be used for a number of purposes, as shown in Section 4.

The steps taken to construct the best fit wind fields are:

1. Wind Field Library Construction: Construct a wind field library using the CFD for the urban area under consideration. Each entry in the wind field library corresponds to a CFD solution found from prevailing conditions that have been imposed as boundary conditions on the CFD model.
2. Response Surfaces Construction: Using the wind field library and the meteorological station locations, construct response surfaces that characterize the response of the stations readings to the prevailing conditions which were used to generate the CFD wind field library.
3. Response Surfaces Fitting: Using a linear-least squares fitting, construct a functional relationship that describes the response surfaces for each of the meteorological stations.
4. Functional Minimization: For each sample time of the meteorological station data, minimize a functional that relates the difference between measured and wind field readings at the stations locations. This functional has as independent variables the prevailing conditions, which when minimized, yields the "best fit" prevailing conditions.
5. Best Fit Wind Fields Construction: Given the "best fit" prevailing conditions, produce individual best fit wind fields from the wind library via interpolation.

The following sections describe the details behind these steps.

2.1 CFD-Urban Model

CFD-Urban is a suite of Computational Fluid Dynamics modeling software that is being used to simulate the wind, turbulence and dispersion fields in urban areas [Coirier et al., 2003.a,b, 2005.a,b,c, 2006.a,b,c]. CFD-Urban has been developed under a program sponsored by the Defense Threat Reduction Agency [Coirier et al., 2003.b], and has been built using parts of a commercially available software suite, CFD-ACE+ [ACE+ 2003]. It solves the Reynolds-Averaged Navier-Stokes equations using a collocated, Finite-Volume method implemented upon structured, unstructured and adaptively-refined grids using a pressure-based approach based upon the SIMPLE algorithm [Jiang, 1994, Jiang, 1999]. Turbulence closure is found by solving a variant of the standard k-ε model [Launder, 1974]. Buildings are modeled either explicitly, by resolving the buildings themselves, and/or implicitly, by modeling the effects of the buildings upon the flow by the introduction of source terms in the momentum and turbulence model equations [Coirier 2003.b]. CFD-Urban solves the steady-state and unsteady Reynolds Averaged Navier-Stokes (RANS) equations, as well as by using a Large Eddy Simulation (LES) approach. Since CFD-Urban solves the governing mass and momentum conservation laws at scales smaller than the buildings

themselves, important urban aerodynamic features are naturally accounted for, including effects such as channeling, enhanced vertical mixing, downwash and street level flow energization.

2.1 Wind Library Construction

The first step is the construction of a wind field library containing CFD produced wind and turbulence fields for the urban area under consideration. Each entry of the wind field library stores the velocity and turbulence fields at all points in the CFD mesh corresponding to a particular set of prevailing conditions that have been applied as boundary conditions. For the cases shown here we use a logarithmic profile for the prevailing wind speed, which uses the following equilibrium relations:

$$U = \frac{u_*}{\kappa}\log(\frac{z}{z_0}) \quad (1)$$

$$k = \frac{u_*^2}{\sqrt{C_\mu}} \quad (2)$$

$$\varepsilon = \frac{u_*^3}{\kappa z} \quad (3)$$

Since we vary the friction velocity, u_*, and the wind direction θ, we can view any quantity taken from the wind library as a function of the two parameter space (u_*, θ). More complex boundary conditions may be parameterized in terms of a larger dimension parameter space.

2.2 Response-Surface Construction

The next step is to compute the Cartesian velocity components (u,v,w) at each meteorological station sites using all of the entries in the wind field library. This produces what we call response surfaces, such as that shown in Figure 2.2.1, which shows contours of u-component of the velocity at a particular meteorological station, plotted against the independent variables (u_*, θ).

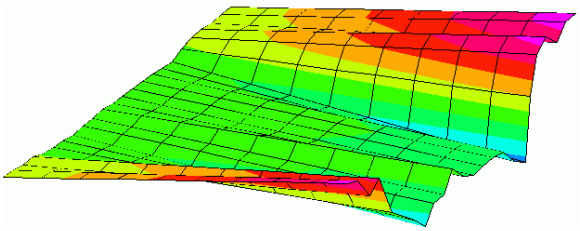

Figure 2.2.1: Sample response surface plotted in (u_*, θ), with the vertical coordinate the u-velocity component.

These response surfaces characterize the velocity component responses to changes in the prevailing conditions using the CFD solution data. The construction of the response surfaces needs to be performed only once, and is essentially a post-processing step of the CFD data contained in the wind field library.

2.3 Response-Surface Fitting

Once the response surfaces have been constructed, a functional form is found that describes the variation of each velocity component at each of the station locations with respect to the parameter space, (u_*, θ). For the work shown here we use linear-least squares fitting with a tensor product set of basis functions in order to find functional forms of the velocity components at each of the m meteorological stations. For the m-th station, the Cartesian velocity component response surfaces may be represented as:

$$u_{m,fit} = \sum_i \alpha_i F_i(u_*, \theta) \quad (4)$$

$$v_{m,fit} = \sum_i \beta_i G_i(u_*, \theta) \quad (5)$$

$$w_{m,fit} = \sum_i \gamma_i H_i(u_*, \theta) \quad (6)$$

The basis functions F, G and H may take different forms, although we use the same forms here for simplicity. Since the parameter space is periodic in θ we use a Fourier series in θ and a polynomial series in u_*. These functional forms of the response surfaces are used in the next step, the functional minimization.

2.4 Functional Minimization

For a given set of meteorological data taken at each of the station sites, we minimize a functional that relates the square-norm of the difference between the measured (meteorological station) and fitted (response

surface) Cartesian velocity components. That is, minimize:

$$S(u_*,\theta)=\sum_m\left[\begin{array}{l}\left(u_m-u_{m,fit}(u_*,\theta)\right)^2+\left(v_m-v_{m,fit}(u_*,\theta)\right)^2+\\ \left(w_m-w_{m,fit}(u_*,\theta)\right)^2\end{array}\right] \quad (7)$$

with respect to (u_*,θ), where the index m varies over all the meteorological station sites. This minimization is performed for each timestamp of the station data, yielding values of (u_*,θ) for each time sampling point. For the work shown here, we use an IMSL routine to perform the minimization. IMSL is a library of FORTRAN subroutines for solving problems in applied mathematics. In this particular case, the IMSL function DUMPOL is used to carry out the minimization [IMSL]. DUMPOL uses the polytope algorithm to find a minimum point of a function f(x) of n variables.

2.5 Best Fit Wind Fields Construction

The functional minimization gives the prevailing conditions (u_*,θ) for each of the timestamps, which is used to construct a corresponding wind field from the wind library entries. For these surface, the wind libraries store data in a two-dimensional space, so we use an iso-parametric quadrilateral finite-element interpolation procedure to interpolate all data from the wind library space given (u_*,θ). To perform the interpolation, we first find the quadrilateral surrounding the point, and then compute the natural coordinates (ξ,η) using an iso-parametric quadrilateral formulation commonly used in Finite Element models. These coordinates are then used to compute the values of all quantities at the given (u_*,θ). The interpolated quantities include primitive variables stored at the Finite-Volume mesh vertices and cell centers as well as mass fluxes at cell interfaces. Processing all of the (u_*,θ) for a given set of met station data produces what we term a "best fit wind library", which is a collection of best fit wind fields found from the minimization procedure.

3. DEMONSTRATION OF APPROACH USING FIELD TEST DATA

We use meteorological sampler data taken during the Joint Urban 2003 Field Test [Allwine et al., 2004] to demonstrate the best fit wind field approach. The Joint Urban 2003 Experiment (JU2003) was conducted between June 28 and July 31, 2003 in Oklahoma City. This extensive field experiment was performed by over a hundred scientists, and was conducted to provide detailed airflow and tracer concentration data to be used to understand the urban area flow and transport and dispersion processes, and to provide model validation data for current and next generation models. During JU2003, researchers installed anemometers in and around the urban area for continuous measurement of airflow during the experiment. Extensive measurements were also made in the Park Avenue Street canyon. An extensive amount of measured data for airflow and tracer concentrations are available from the web site https://ju2003dpg.dpg.army.mil.

3.1 Demonstration of approach using IOP2, IOP3 and IOP9

For the study here, we use data from twenty Super Portable Weather Information Display (PWIDS) systems that were fielded for the field test. All of these PWIDS stations were located in the Central Business District (CBD) of Okalahoma City and all sensors were mounted approximately 8m above the street level. Figure 3.1.1 shows the PWIDS locations in the Oklahoma City CBD. To demonstrate the best fit approach, we use the 10 minutes averaged Dugway Proving Ground PWIDS data for IOP2, IOP3 and IOP9.

Figure 3.1.1: DPG PWIDS Sampler Locations for JU2003.

As noted above, the first step is to construct a wind field library. CFD-Urban was used to generate a quadtree/prismatic mesh with approximately 500,000 cells in the OKC CBD, yielding a resolution on the ground plane of approximately 7 meters. Figure 3.1.2 shows an overview of the mesh.

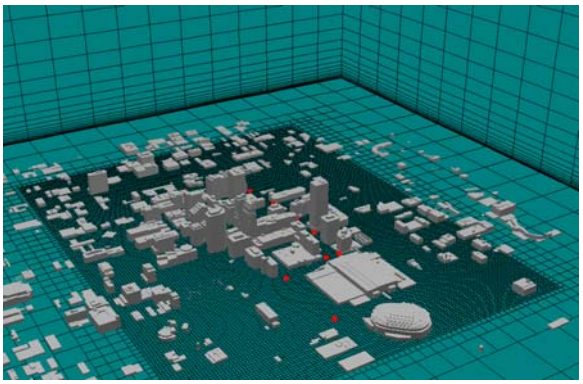

Figure 3.1.2: Overview of the CFD-Urban generated mesh for the best fit library study.

The wind field library was constructed using the logarithmic velocity and turbulence profiles noted in equations (1-3) as boundary conditions for friction velocities ranging from 0.1 m/s to 1.0 m/s in steps of 0.1 m/s and prevailing flow directions ranging over 360 degrees in 30 degree increments. This yields a library containing 120 unique entries. Response surfaces were constructed and fitted for each of the 20 PWIDS stations locations using the wind library entries as noted in Section 2.2 and 2.3. Figure 3.1.3 shows sample response surfaces from the wind library for PWIDS sensor 19.

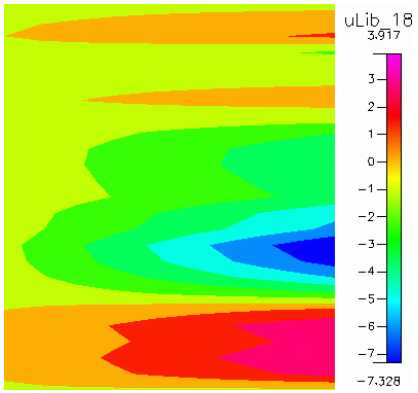

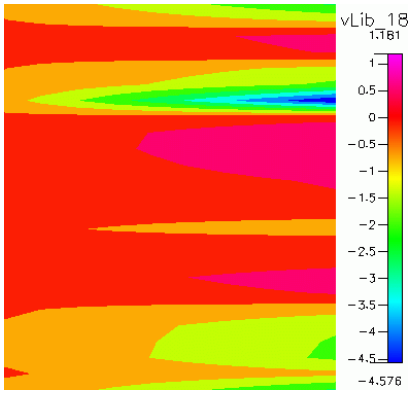

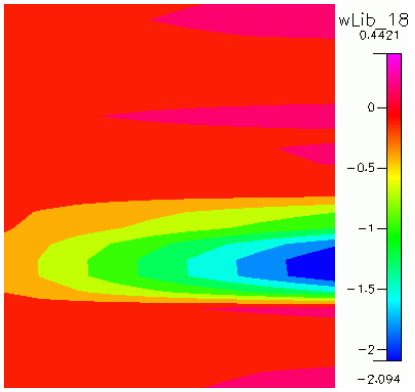

Figure 3.1.3: Sample response surfaces in the (u_*, θ) space for PWIDS sensor 18 showing the Cartesian velocity components, u,v and w (top to bottom in figure).

For each of the 3 Intensive Operating Periods evaluated (IOP2, 3 and 9), we processed the PWIDS data and performed the minimization procedure noted in Section 2.4 for each timestamp in the PWIDS data files. This produces (u_*, θ) at each of the timestamps for each of the IOP datasets. Figure 3.1.4 shows the friction velocity for all three IOP datasets, while Figure 3.1.5 shows the prevailing wind directions.

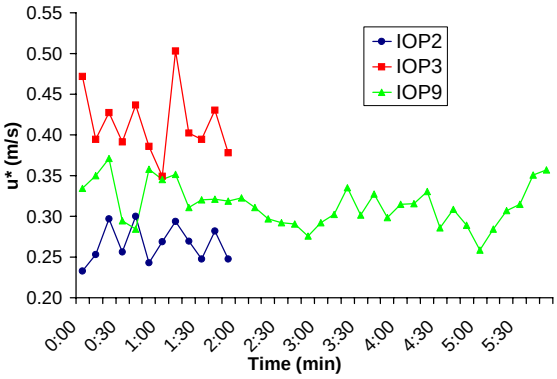

Figure 3.1.4:. u at 10 minute intervals for IOP2, IOP3 and IOP9.*

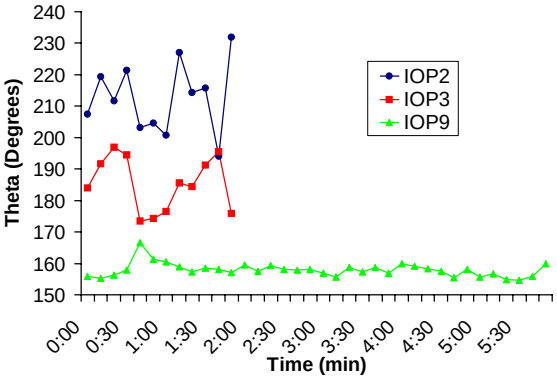

Figure 3.1.5: θ at 10 minute intervals for IOP2, IOP3 and IOP9.

In order to evaluate how well the best fit approach is performing, we compute wind speed and wind direction errors by comparing the best fit to the measured data for each time at each station for the three IOPs. We define the wind speed and wind direction error at the t[th] timestamp for the m[th] PWIDS station as:

$$\varepsilon_{U,mt} = \left| U_{mt} - \hat{U}_m(u_*,\theta)_t \right| \quad (8)$$

$$\varepsilon_{\theta,mt} = \left| \theta_{mt} - \hat{\theta}_m(u_*,\theta)_t \right| \quad (9)$$

where $\hat{U}_m(u_*,\theta)_t$ and $\hat{\theta}_m(u_*,\theta)_t$ are the best fit wind library wind fields wind speed and direction evaluated at the m[th] PWIDS sensor using the t[th] time stamped best fit wind field. Using these, the mean wind speed and wind direction errors for a given PWIDS station are:

$$\bar{\varepsilon}_{U,m} = \sum_{t=1}^{N} \frac{\varepsilon_{U,mt}}{N} \quad (10)$$

$$\bar{\varepsilon}_{\theta,m} = \sum_{t=1}^{N} \frac{\varepsilon_{\theta,mt}}{N} \quad (11)$$

Table 1 shows the average mean errors and average root mean square errors of wind speed and wind direction for all three IOPs, where the averaging is taken over all PWIDS stations. Figure 3.1.6 plots the mean wind speed error for each station for the three IOPs, while Figure 3.1.7 plots the mean wind direction error. Figure 3.1.8 shows the normalized mean wind speed error at all the PWIDS stations for the 3 IOPs.

IOP	$\bar{\varepsilon}_U$ (m/s)	$\bar{\sigma}_U$ (m/s)	$\bar{\varepsilon}_\theta$ (deg)	$\bar{\sigma}_\theta$ (deg)
2	0.761	0.079	0.983	0.080
3	1.150	0.081	1.058	0.122
9	1.041	0.036	1.180	0.063

Table 1: Average mean errors and average root mean square errors of wind speed and direction for the three IOPs.

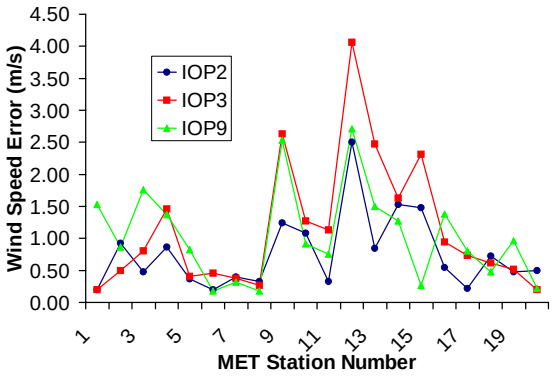

Figure 3.1.6: Mean wind speed error at all PWIDS stations for IOP2, IOP3 and IOP9.

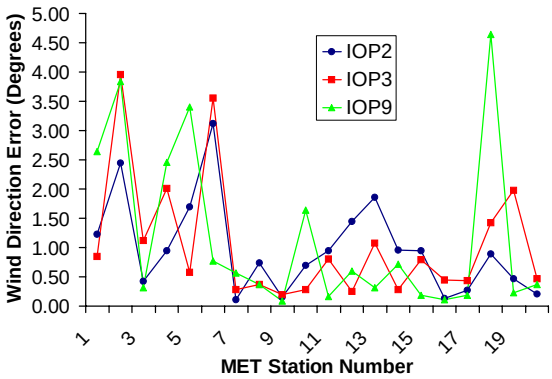

Figure 3.1.7: Mean wind direction error at all PWIDS stations for IOP2, IOP3 and IOP9.

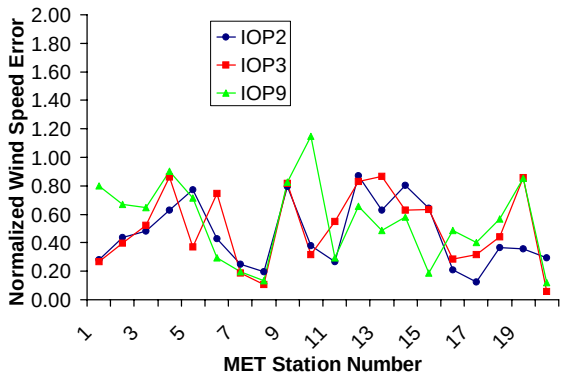

Figure 3.1.8: Normalized mean wind speed error at all PWIDS stations for IOP2, IOP3 and IOP9.

Inspection of these plots and table indicates that the best fit wind field construction performs reasonably well, although there is room for improvement. The wind directions are fit quite well, as seen in Table 1, with a mean error of approximately 1 degree, although the wind speeds are not fit as well. This may be caused by some deficiency in the CFD model data, or could be alleviated by using a different functional to minimize. These will be investigated further.

4. USE OF BEST FIT WIND FIELDS FOR SENSOR SITING IMPROVEMENT AND CHARACTERIZATION

Once the best fit wind fields and response surfaces have been constructed, there are a variety of techniques that may be exploited to help site sensors and characterize and correlate sensor readings. These correlations may be made with the prevailing conditions, to other sensors as well as to conditions at locations where there are no sensors. As an example, this may be used to find a functional relationship between rooftop level wind readings and street level conditions. Furthermore, since the best fit approach yields a wind library of the best fit wind fields, these wind fields may be used to perform CFD-based transport and dispersion calculations using boundary conditions that are more representative of those actually ocurring during the test. The following sections illustrate examples of these potential uses for the approach.

4.1 Sensor-to-Prevailing Conditions Correlations

Using the wind field libraries, we can reconstruct the response of sensors to prevailng locations, taking into account the influence of the local buildings. These correlations are derived from the response surface plots that are generated from the wind library. Shown below are two polar plots which show the local wind speed response as a function of the prevailing wind direction. In these plots, the radius is the normalized wind speed, while the angle is the prevailing flow direction θ. The normalized wind speed is defined as:

$$\tilde{U} = \frac{U}{U_\infty(z_m)} \qquad (12)$$

where

$$U_\infty(z_m) = \frac{u_*}{\kappa}\log\left(\frac{z_m}{z_0}\right) \qquad (13)$$

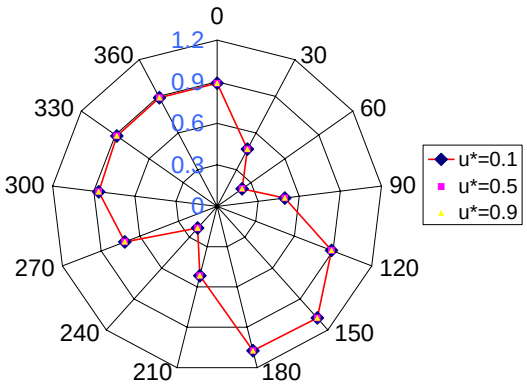

Figure 4.1.1: Polar plots of normalized local wind speed at PWIDS station 2.

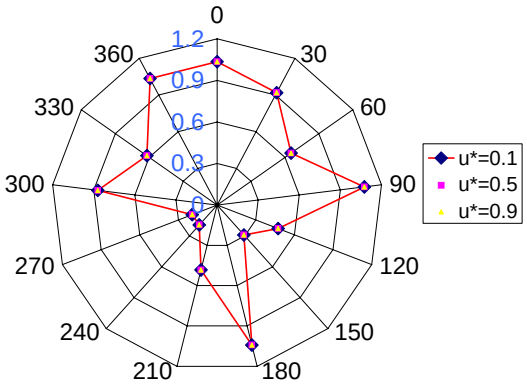

Figure 4.1.2: Polar plots of normalized local wind speed at PWIDS station 20.

4.2 Sensor-to-Street Level Conditions Correlations

One outcome of the best fit library construction is the ability to correlate conditions at locations in the urban where there are no sensors to locations where there are sensors. An example of this is shown below using the

Oklahoma City wind libraries for illustrative purposes.

Consider Figure 4.2.1, which shows 5 street level sensors (in green) and one rooftop sensor (in red). The three sensors roughly aligned with the street are in the Park Avenue street canyon, while the rooftop sensor is located on top of the Sonic building, which is approximately 150 meters AGL. Located immediately to the North and South of the Sonic building at street level are two sensors that are directly influenced by the large downwash and upwash induced by the tall building.

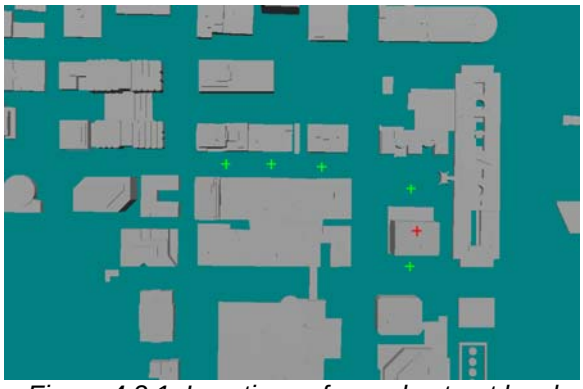

Figure 4.2.1: Locations of sample street level (green) and roofttop (red) sensors to illustrate how one can correlate rooftop to street level winds.

Figures 4.2.2 and 4.2.3 shows how street level wind speeds and directions at the three Park Avenue locations can be inferred as functions of the readings at the rooftop sensor. The street channel switching is prominently shown in Figure 4.2.3.

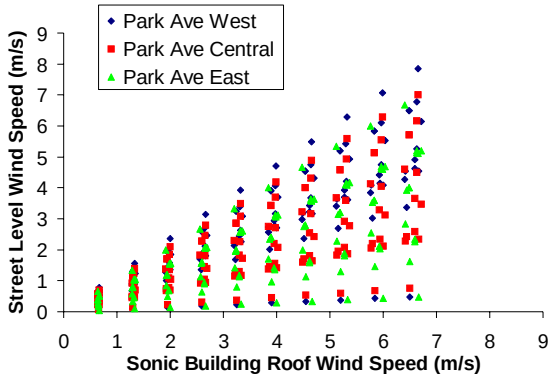

Figure 4.2.2: Rooftop versus Park Avenue Canyon wind speed correlation.

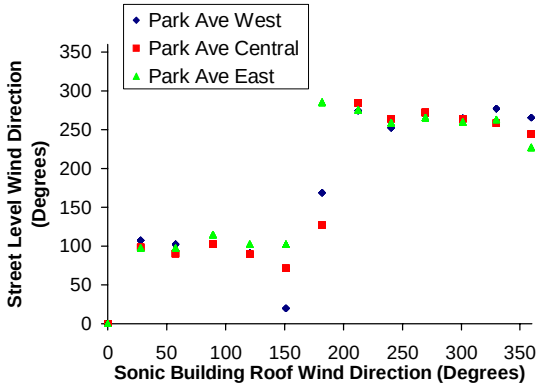

Figure 4.2.3: Rooftop versus Park Avenue Canyon wind direction correlation.

The influence of isolated tall buildings has been shown to have a first-order impact upon the street-level winds, and corresponding transport and dispersion behavior near the buildings in recent fields tests conducted in New York City [Camelli, et al., 2006, Coirier, et al., 2006.b]. Figures 4.2.4 and 4.2.5 show how the street level wind speed and direction may be correlated to the local rooftop readings.

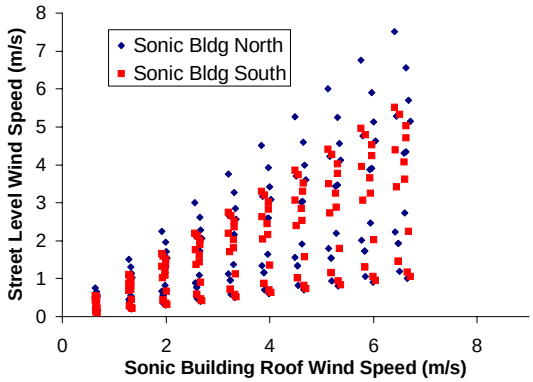

Figure 4.2.4: Rooftop versus street level wind speed correlation.

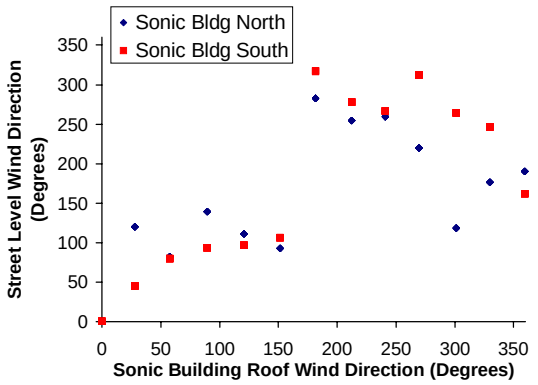

Figure 4.2.5: Rooftop versus street level wind direction correlation.

4.3 T&D Using Best Fit Wind Library

As noted above, the outcome of the approach presented here is a library of "best fit" wind fields. These may be used directly to perform transport and dispersion calculations using the frozen hydrodynamics approach described in [Coirier, et al., 2006.b]. This approach solves unsteady Eulerian transport equations using the wind and turbulence fields contained in the wind library, by blending the wind fields in time. Since these wind fields have been constructed using the intra-urban meteorological stations data, the premise is that this will improve the transport and dispersion modeling accuracy.

Transport and dispersion calculations with a release rate and location corresponding to the actual tracer gas released during IOP9 were performed using CFD-Urban, where the best fit wind field library for this IOP was used to provide the wind fields. Figure 4.3.1 shows the predicted maximum ground level concentrations found when using the best fit approach. The measured values are also shown as point data in these plots.

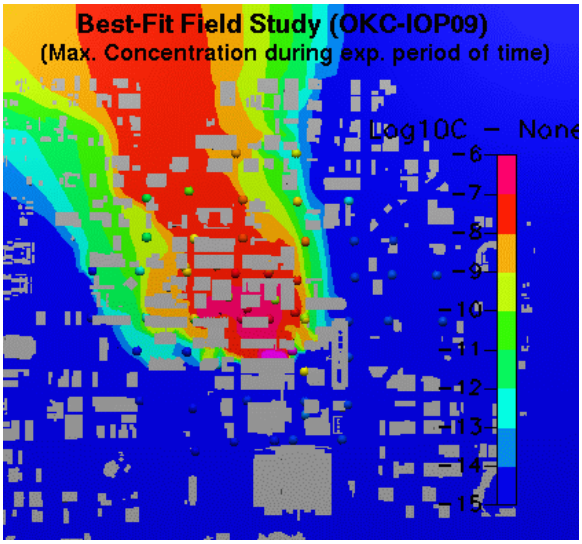

Figure 4.3.1: Calculated maximum ground concentration values for IOP9 using the best fit wind field library.

4.4 Sensor Siting Sensitivities

In general, one would like to know locations in the urban area that are more closely correlated to the prevailing conditions. Building wakes and upwash/downwash regions have a direct impact upon these correlations, and these phenomena change with different prevailing conditions. Here we demonstrate one technique that uses the best fit wind library to produce maps that show the averaged deviation of the local flow wind speed and direction from the prevailing conditions. Using each entry in the wind library, we compute:

$$\delta_U = \frac{|U_\infty - U|}{U_\infty} \qquad (14)$$

$$\delta_\theta = |\theta_\infty - \theta| \qquad (15)$$

at each point for each prevailing condition, and then average these quantities and plot contours of the averages. Inspection of these contours can reveal locations where the local conditions are more representative of the prevailing conditions, which can aid in siting the sensors. Figure 4.4.1 and 4.4.2 show these contours in the Oklahoma City CBD at the PWIDS stations heights of 8 meters.

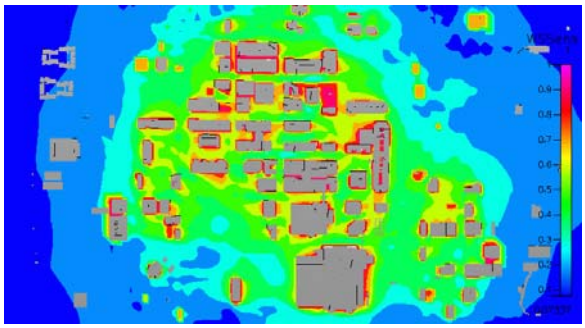

Figure 4.4.1: Contours of $\overline{\delta}_U$ at z=8m AGL.

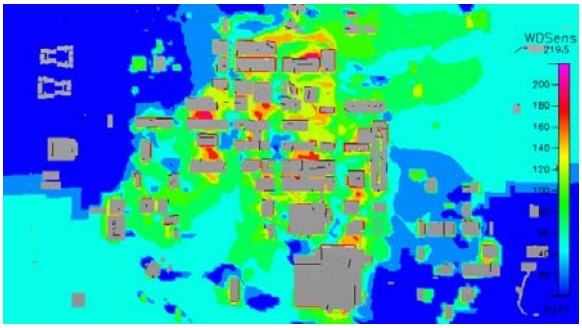

Figure 4.4.2: Contours of $\overline{\delta}_\theta$ at z=8m AGL.

5. CONCLUSIONS

We have demonstrated a technique that may be used to help site and improve the quality of readings from intra-urban sited meteorological stations. The approach is based upon using high-resolution CFD-generated wind fields in conjunction with the measured meteorological stations data to produce "best fit" wind fields. These high-resolution CFD-based fields are found by minimizing a functional that describes the difference between the measured and computed fields. In order to perform this minimization, response surfaces are generated at each station that relates the computed velocity field to the (prescribed) prevailing conditions. These surfaces are then used during the functional minimization at each time period in which meteorological data is available. Once these best fit fields are found, a variety of techniques have been explored in that may be used to improve the sensor readings quality.

In this paper we have outlined the steps taken to perform the best fit wind field construction, and have demonstrated it using meteorological stations data taken during the Joint Urban 2003 field test. We have shown how sensors may be correlated to the prevailing conditions, and have shown how sensor readings may be correlated to locations where there are no sensors, such as correlating rooftop to street level winds. We have shown how the approach may be directly used to improve transport and dispersion modeling accuracy, and how the sensitivities of sensor location may be displayed in a city, which may be used to help site sensor to improve their performance.

6. ACKNOWLEDGEMENTS

The authors gratefully acknowledge the support for this work, that was funded under a Small Business Innovation Research Phase I grant through the Defense Threat Reduction Agency, Technical Monitor, CDR Stephanie Hamilton/USN.

7. REFERENCES

ACE+: CFD-ACE+, V2003 Users Manual, Volumes 1 and 2.

Allwine, K.J., et al., 2004: "Overview of Joint Urban 2003- an atmospheric dispersion study in Oklahoma City." Symposium on Planning, Nowcasting, and Forecasting in the Urban Zone, January 11-15, Seattle, WA, Amer. Met. Soc., Boston, MA.

Allwine, K.J., J.H.Shinn, G.E. Streit, K.L. Clawson, M.Brown, 2002, Overview of Urban 2000. Bull. Am. Meteorol. Soc., 83 (4), 521-536.

Boris, J.P., "Dust in the Wind: Challenges for Urban Aerodynamics:, AIAA-2005-5393.

Coirier, W., Kim, S., 2004: Validation of CFD-Urban using Accepted Open Field and Urban Area Transport and Dispersion Test Data. 8th Annual George Mason University Conference on Transport and Dispersion Modeling, July 13-15, Fairfax, Virginia.

Coirier, W., Reich, A., Fricker, D., Furmanczyk, M., Przekwas, A., 2003.a: Application of CFD-Urban For Support of the Joint URBAN 2003 Field Test, 7th Annual George Mason University Conference on Transport and Dispersion, Fairfax, Virginia.

Coirier, W.J., Fricker, D.M., and Furmanczyk, M.: 2003.b, Development of a high fidelity PC based simulator for modeling the atmospheric transport and dispersion of nuclear, chemical, biological and radiological substances in urban areas, DTRA SBIR Phase II Final Report: Contract: DTRAA01-01-0079

Coirier, W.J., Fricker, D.M., Furmanczyk, M., and Kim, S.: 2005.a. “A Computational Fluid Dynamics Approach for Urban Area Transport and Dispersion Modeling”, in print, Environmental Fluid Mechanics, Vol. 15(5).

Coirier, W.J., Kim, S. 2006.c. Summary of CFD-Urban Results in Support of the Madison Square Garden and Urban Disperison Program Field Tests, American Meteorological Society, 6th Symposium on the Urban Environment.

Coirier, W.J., Kim, S., 2005.b: Recent developments and applications of the cfd-urban transport and dispersion model, 9th Annual George Mason University Conference on Transport and Dispersion Modeling, July 18-20, Fairfax, Virginia.

Coirier, W.J., Kim, S., 2005.c: Detailed transport and dispersion calculations in support of the MSG05 field test, 9th Annual George Mason University Conference on Transport and Dispersion Modeling, July 18-20, Fairfax, Virginia.

Coirier, W.J., Kim, S., Chen, F., Tuwari, M.,: 2006.a. Evaluation of urban scale contaminant transport and dispersion modeling using loosely coupled CFD and mesoscale models, American Meteorological Society, 6th Symposium on the Urban Environment.

Coirier, W.J., Kim, S.K, 2006.b, CFD Modeling for Urban Area Contaminant Transport and Dispersion: Model Description and Data Requirements, American Meteorological Society, 6th Symposium on the Urban Environment, 2006.

Hanna, S.R., White, J., Zhou, Y, Kosheleva, A., Analysis of Joint Urban 2003 (JU2003) and Madison Square Garden 2005 (MSG05) Meteorological and Tracer Data, 2006: Paper J7.1 American Meteorological Society, 6th Symposium on the Urban Environment.

http://www.vni.com/products/imsl/documentation/index.html#fort

IMSL MATH/LIBRARY User's Manual,

Jiang, Y., Fricker, D.M., Coirier, W.J.: 1999, Parallelization of a fully implicit unstructured pressure-based flow solver using MPI, AIAA-99-3274.

Jiang, Y., Przekwas, A.J.: 1994, Implicit, pressure-based incompressible Navier-Stokes solver for unstructured meshes, AIAA-94-0303.

Launder, B.E. and Spalding, D.B.: 1974, The numerical computation of turbulent flows, Computer Methods in Applied Mechanics and Engineering. 3, 269-289.

Oke, T.R., Observing urban weather and climate using 'standard' stations; http://www.meteo.bg/EURASAP/35/paper1.html

Smith, W.S., Brown, M.J., 2002, “A CFD-Generated Wind Field Library Feasibility Study: Maximum Wind Direction Interval”, LA-UR-02-1100, also in the AMS 4th Symposium on the Urban Environment, Norfolk, VA.

UDP, DHS/DTRA Urban Dispersion Program studies, available on the web via http://urbandispersion.pnl.gov/

Weil, J.C., Sykes, R.I., and Venkatram, A.: 1992, Evaluating air-quality models: review and outlook, Journal of Applied Meteorology, 31, 1121-1145.

WMO, 1983a, Guide to Meteorological Instruments and Methods of Observation, 5th Edn. WMO, Geneva.

WMO, 1983b, Guide to Climatological Practices, 2nd edn, WMO-No-100, WMO, Geneva.